David Jang

Reprinted from May 1977, Vol. 99, Journal of Pressure Vessel Technology

The Inelastic Deformation of Pressurized Stainless Steel Tubes Under Dynamic Bending and Torsional Loading

L. D. LARSON

Section Manager,
Bettis Atomic Power Laboratory,
Westinghouse Electric Corporation,
West Mifflin, Pennsylvania
Mem. ASME

W. F. STOKEY

Associate Professor,
Department of Mechanical Engineering,
Carnegie-Mellon University,
Pittsburgh, Pennsylvania
Mem. ASME

A test program was conducted to investigate the inelastic response behavior of internally pressurized tubes subjected to dynamic bending and torsion loads. The basic experiment was a drop test in which the cantilever tube was dynamically loaded by a torque arm with a concentrated weight at the end. The experimental data consist of strain versus time records and peak and permanent deflections. Analytical predictions of the response were made using a lumped parameter beam model of the structure. This simple representation of the pressurized tube is made possible by use of an approximate analytical model for the inelastic deformation of a pipe element subjected to pressure, bending and torsion. The predicted responses are compared with measured responses to assess the accuracy of the models.

Introduction

A problem of interest to the nuclear industry in the evaluation of the consequences of certain postulated accident conditions is the response of pressurized pipes to dynamic loads which are severe enough to cause large inelastic deformations. Section III of the ASME Boiler and Pressure Vessel Code [1][1] provides rules for the evaluation of the results of "Faulted Conditions," which are extremely-low-probability postulated events. For example, in a piping system an assessment of the consequences of pipe whip following a rupture in the pipe might be required.

This paper presents the results of experiments that were performed to investigate the inelastic behavior of pressurized tubes under dynamic loading. Tubes made of Type 304 stainless steel were pressurized to stress levels normally permitted in the design of piping for reactor systems, and subjected to drop tests which caused significant plastic deformation under the dynamically induced bending and torsional loads. The tests yielded strain versus time records and measurements of peak and permanent deflections. Analytical predictions were made using a step by step numerical integration of the equations of motion for a lumped parameter representation of the tube.

In an earlier paper [2], the authors described an approximate model for the elastic-plastic analysis of a pipe element under combined loading. It was shown that the model gave good predictions of deformation in Type 304 stainless steel tubes subjected to combined loadings applied statically. The incentive for developing the simplified model was for application to dynamic loading of piping systems into the plastic strain range. Because of the nonlinearity of such systems, the equations of motion must be integrated in a stepwise fashion, considering all loads simultaneously. Conceptually, with the use of digital computers, such step by step integration can be accomplished. However, there is a practical limitation to the number of degrees of freedom that can be handled in a given problem. For a three dimensional piping system it is desirable, at least in preliminary analysis, to be able to deal with gross beam elements as in the elastic analysis. In this paper, analytical predictions based on the simplified model are compared with the experimental results obtained from dynamic loading of pressurized, cantilevered tubes.

Test Procedure

The tubes were loaded by drop testing, using the apparatus shown in Fig. 1. The tube being tested is supported as a cantilever by the clamping fixture mounted on the test carriage, which is guided by two vertical rods on 24-in. (60.96-cm) centers. The quick release mechanism at the top of Fig. 1 is supported by a line which passes through a pulley, so that the drop height can be readily adjusted. The tube is pressurized with oil supplied through the flexible pressure line. The torque arm which is clamped to the tube, has a weight on its end, and applies the inertial bending and torsional loads. The motion of the test carriage is arrested at the bottom of its fall by small lead plates, which stop the carriage motion suddenly, with very little rebound. These plates are placed at the nodal points for free-free

[1] Numbers in brackets designate References at end of paper.

Contributed by the Pressure Vessels and Piping Division and presented at the Petroleum Mechanical Engineering and Pressure Vessels and Piping Conference, Mexico City, Mexico, September 19-24, 1976, of THE AMERICAN SOCIETY OF MECHANICAL ENGINEERS. Manuscript received at ASME Headquarters, May 24, 1976. Paper No. 76-PVP-24.

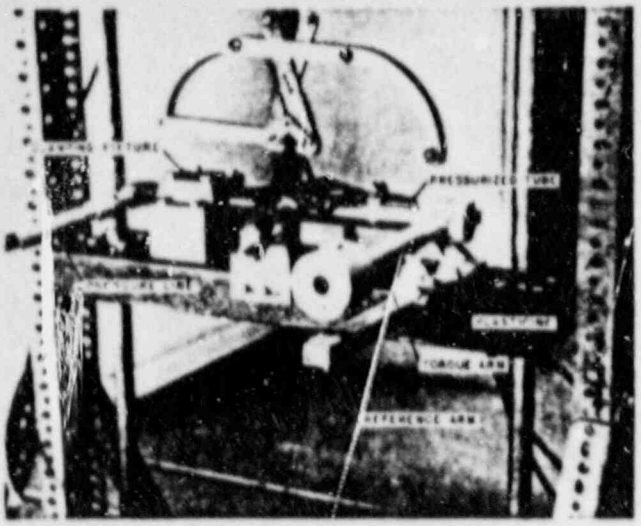

Fig. 1 Drop test setup

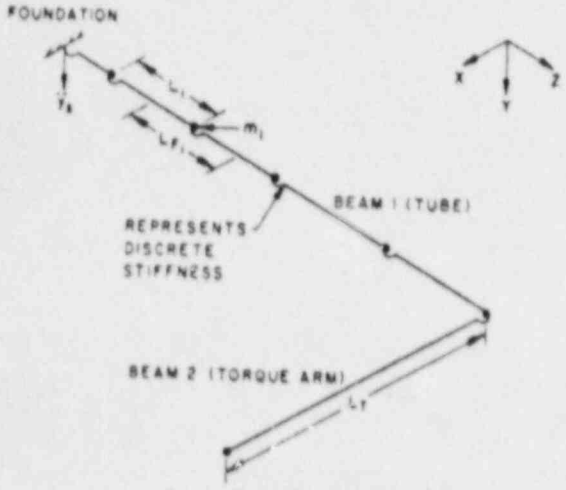

Fig. 2 Dynamic analysis model

vibration of the carriage in its fundamental mode, as determined by test.

Post yield resistance strain gages were mounted with various orientations on the outer surface of the tube near its supported end. The gages were connected to amplifiers, the outputs of which were recorded on a Visicorder using four galvanometers having a frequency response of 0–1000 cps, and one having a response of 0–4800 cps.

To measure the peak dynamic deflections, pieces of plasticine were placed on the test carriage and on a reference arm located under the torque arm. The initial gaps between the plasticine and the bottom of the torque arm were such that the plasticine was contacted and deformed during a test. Permanent deflections were found using appropriate measurements.

Specimens

The test specimens were machined from pieces of extruded seamless tube having an inside diameter of 1.007 in. (2.56 cm). A test length of 4 in. (10.16 cm) or 10 in. (25.4 cm) was machined to a wall thickness of 0.05 in. (0.127 cm) or 0.100 in. (0.254 cm). The supported end which fitted into the clamping fixture had an outside diameter of 1.275 in. (3.24 cm) and a length of 3 in. (7.62 cm), while the loading end had the same outside diameter

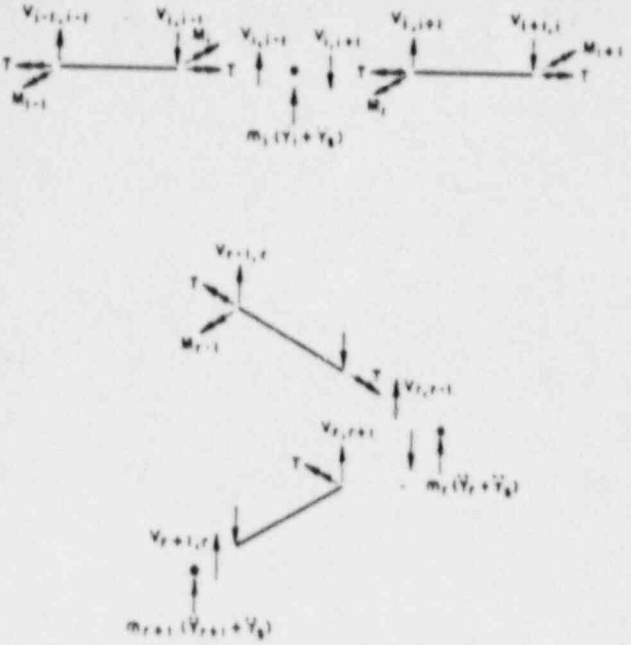

Fig. 3 Equilibrium of element free bodies

and a length of 2 in. (5.08 cm). The material was annealed, after machining, to remove residual stresses. While the heat treatment caused some bowing of the specimen, the wall thickness remained uniform, since no machining was done after the heat treatment. Tensile tests were conducted on specimens, which had been subjected to the same heat treatment, to determine the stress-strain behavior. A plug with a hole in it, through which the pressurizing oil was supplied, was placed in the supported end of the tube. A solid plug was placed in the other end. These plugs were tack welded to the tube to seal the oil.

Analysis

The use of the pipe element described in reference [2] permits the structural model to be reduced to a simple beam structure. In the dynamic analysis, the lumped parameter model shown schematically in Fig. 2 was used to represent the pressurized tube and the torque arm. The direction of shock is normal to the plane of the model. The pressurized tube, represented by Beam 1, was subdivided into a number of massless rigid links connected by flexible joints, which represent the flexibility of length L_i concentrated at point i. Spacing of the joints was varied with smaller lengths used near the support where the highest deformations occurred. The mass m_i concentrated at the joint i represents the mass of the tube and fluid contained within it, of the length attendant to the joint. The torque arm is represented by a single flexible element of length L_T, since its behavior was elastic during all tests.

The forces acting on element free bodies are shown in Fig. 3. Using equilibrium of the massless links to obtain the shear forces in terms of moments and torques and substituting these into Newton's second law for the mass point yields, for $i < r$, r being the number of elements in Beam 1:

$$\ddot{y}_i = \frac{1}{m_i}\left(-\frac{M_{i-1}}{L_i} + \frac{(L_i + L_{i+1})M_i}{L_i L_{i+1}} - \frac{M_{i+1}}{L_{i+1}} \right) - \ddot{y}_i \qquad (1)$$

where m_i = mass of ith element

$\ddot{y}_i$ = acceleration of the mass relative to the foundation

$\ddot{y}_s$ = foundation acceleration

For the last mass on the tube:

$$\ddot{y}_r = \frac{1}{m_r}\left(- \frac{M_{i-1}}{L_r} + \frac{T}{L_T}\right) - \ddot{y}_s \tag{2}$$

where m_r equals mass of last element of tube plus additional mass of clamping fixtures. For the element representing the torque arm:

$$\ddot{y}_{T+1} = \frac{1}{m_{T+1}}\left(- \frac{T}{L_T}\right) - \ddot{y}_s \tag{3}$$

where m_{T+1} equals the mass of torque arm plus mass of weight added to the end.

Integration of the equations of motion was performed using the following finite difference equations [3] to express the deflection and its time derivations, where n is the nth time step:

$$y_i(t_n) = y_i(t_{n-1}) + \dot{y}_i(t_{n-1})\Delta t + 0.5\,\Delta t^2\ddot{y}_i(t_{n-1}) \tag{4a}$$

$$\dot{y}_i(t_n) = \dot{y}_i(t_{n-1}) + 0.5\,\Delta t[\ddot{y}(t_{n-1} + \ddot{y}_i(t_n)] \tag{4b}$$

A time step $\Delta t = 0.000001$ sec was used.

It is assumed that on impact at the end of the drop the foundation motion is arrested in a time inverval t_d by a constant acceleration, yielding:

$$\ddot{y}_s = -\sqrt{2g\bar{h}/t_d} \qquad t < t_d \tag{5a}$$

$$\ddot{y}_s = 0 \qquad t > t_d \tag{5b}$$

The displacement configuration at the end of a time step is known and the change of curvature at a joint i can be determined from the central difference equation:

$$dK_i = \left(\frac{dy_{i-1}}{L_i} - \frac{(L_i + L_{i+1})}{L_iL_{i+1}}\,dy_i + \frac{dy_{i+1}}{L_{i+1}}\right)\frac{1}{(L_I)_i} \tag{6}$$

Since rotational inertia of the tube is neglected, the torque T is considered to be uniform along Beam 1.

The change in the angle of twist at the end of the tube is the sum of the changes for the elements:

$$d\beta_r = \sum_{i=1}^{r}(dK_{id})_i(L_I)_i \tag{7}$$

which may also be expressed as:

$$d\beta_r = \left(dy_{r+1} - dy_r - \frac{L_T^2dT}{3EI_1}\right)\frac{1}{L_T} \tag{8}$$

where the third term represents the deflection caused by the bending of the elastic torque arm.

The coefficients for the equations for the deformation of a tube element, as derived in reference [2], are given in the Appendix. The equations are of the form:

$$dK = \frac{\pi}{8R^3h}(A_{11} + B_{11})dM + \frac{\sqrt{3}}{4R^3h}(A_{14} + B_{14})dT \tag{9a}$$

$$dK_{id} = \frac{\sqrt{3}}{4R^3h}(A_{41} + B_{41})dM + \frac{2}{2\pi R^3h}(A_{44} + B_{44})dT \tag{9b}$$

where K = curvature of the tube

K_{id} = angle of twist per unit length

A_{mn} = elastic coefficients

B_{mn} = plastic coefficients

M = applied bending moment

T = applied torque

For element i, omitting coefficients which are zero, equations (9a) and (9b) become:

$$dK_i = \frac{\pi}{8R^3h}(A_{11} + B_{11})_i dM_i + \frac{\sqrt{3}}{4R^3h}(B_{14})_i dT \tag{10a}$$

$$dK_{id_i} = \frac{\sqrt{3}}{4R^3h}(B_{41})_i dM_i + \frac{3}{2\pi R^3h}(A_{44} + B_{44})_i dT \tag{10b}$$

Solving equation (10a) for dM_i, substituting into equation (10b), and using equations (6), (7), and (8) yields:

$$dT = \frac{\dfrac{dy_{r+1} - dy_r}{L_{r+1}} - \dfrac{2\sqrt{3}}{\pi}\displaystyle\sum_{i=1}^{r}\frac{(B_{41})_iL_i}{(A_{11} + B_{11})_i}\,dK_i}{\dfrac{3}{2\pi R^3h}\displaystyle\sum_{i=1}^{r}\left(A_{44} + B_{44} - \frac{B_{41}^2}{A_{11} + B_{11}}\right)L_i + \frac{L_T}{3EL_T}} \tag{11}$$

Thus, the change of torque can be found in terms of known quantities and the change in bending moments at the joints is then found from equation (10a).

Immediately prior to the application of the dynamic load, the tube is stressed only by internal pressure. The dynamic disturbance is introduced in the form of a rectangular deceleration pulse of very short duration applied to the foundation. Thus the velocity, the acceleration, and the stress state for each tube element are known at the start of the transient. The values of these variables, and of the displacement, after each successive time step are found by the following sequence of operations:

1 The finite difference form of the equations of motion are solved for the time step, giving a new displacement configuration for the system.

2 From this, the changes of the curvature and the angle of twist are calculated for each tube element.

3 The new state of stress for each tube element is determined from the approximate tube deformation model, new internal forces are calculated and the force system acting on each lumped mass is updated.

4 A new acceleration and velocity is calculated for each mass, and the process is repeated from Step 1.

Since the pipe element analytical model of reference [2] is formulated in terms of the stress resultants and their associated generalized strains, the physical strains at any point in the cross section must be obtained by assuming a reasonable strain distribution. The elastic strain increments are readily obtained from the classical assumptions. In this analysis, the plastic strain vector is assumed to vary linearly from the neutral axis to the outer fibers. The plastic bending strain increments then vary linearly across the tube and are tension on one side of the neutral axis and compression on the other. The hoop and torsional strain increments also vary linearly but have the same sign in both regions. Transformation matrices relating physical strains to the generalized strains are presented in reference [4].

Results

Table 1 summarizes the test variables for six tests performed. For the pressurized tubes, the initial hoop stress was approximately 60% of the static yield stress of the material. Fig. 4 shows experimental and calculated strains for Test 1 in which bending and torsion were applied dynamically to a pressurized tube. The bottom curves show the bending strain obtained from longitudinal strain measurements on the top and bottom surfaces at a location 0.75 in. (1.91 cm) from the clamped end. These strain magnitudes differed by less than 10 percent from the bending strain magnitudes shown. The bending strain response shows the double peaks that are characteristic of systems in which two natural modes of vibration predominate. This is

Table 1 Test parameters

Test	Tube length (in.)	Wall thickness (in.)	Drop height (in.)	Pressure (psi)	Loading
1	10 (25.4 cm)	0.050 (0.127 cm)	24 (60.96 cm)	2500 (17,200 kPa)	Bending and torsion
2	10	0.100 (0.254 cm)	48 (121.92 cm)	5000 (34,500 kPa)	Bending and torsion
3	10	0.100	48	0	Bending and torsion
4	4 (10.16 cm)	0.050	48	2500	Bending and torsion
5	4	0.060	48	0	Bending and torsion
6	10	0.100	48	5000	Bending

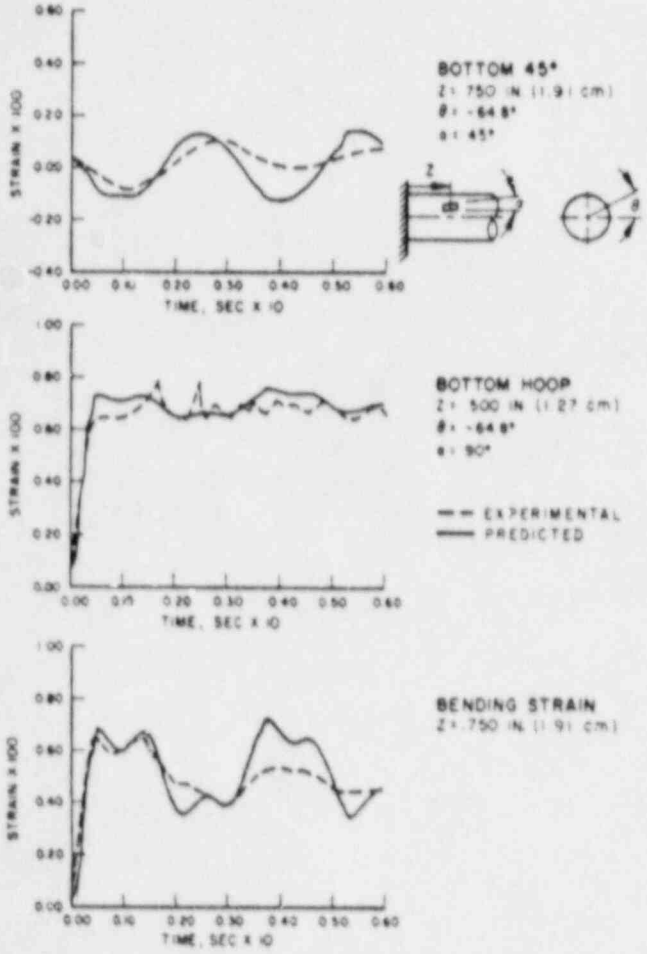

Fig. 4 Predicted and measured response for test no. 1

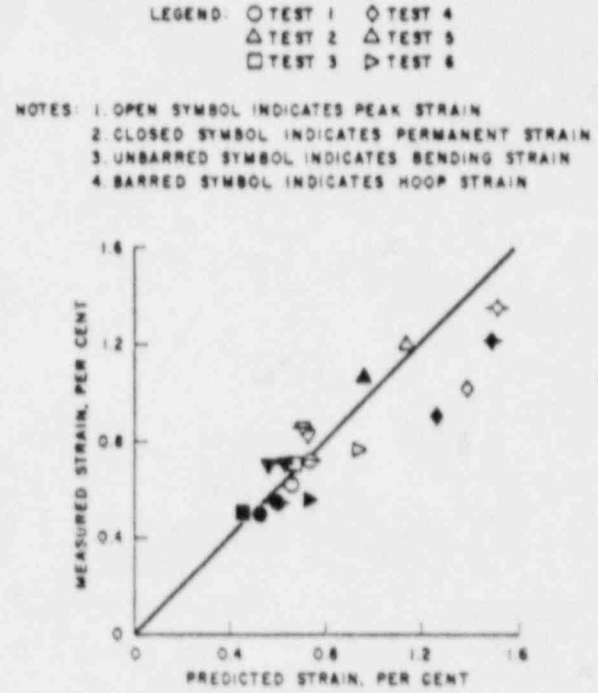

Fig. 5 Comparison of predicted and measured strains

typical of the tests in which both bending and torsion were applied. In this type test, initial yielding is caused primarily by the mass on the end of the tube which moves with a higher frequency than the mass on the end of the torque arm. This mass reverses direction before the mass on the end of the torque arm causing some unloading followed by a second peak. The middle curves show the hoop strain responses at an angular location 64.8 deg from the tube midplane. Hoop strain response curves on the bottom side were typically very flat although some "noise" is present in the experimental curve shown. Tensile hoop strains on the bottom side (which is initially loaded in compression longitudinally) were of about the same magnitude as the bending strains while hoop strains on the top side were quite small. This is due to the different stress states in the two regions. The top curves in Fig. 4 show the responses of a gage located on the bottom side at a location 64.8 deg from the tube midplane and oriented at 45 deg to the tube axis. The response reflects the torsional load and little evidence of the higher frequency mode is present in either the calculated or experimental response curves.

Since no damping was included in the analysis, the agreement between the calculated and experimental response curves is reasonable only for the first cycle. Also, the correction factor applied to the static material properties to account for high strain rate effect was based on the initial strain rate only and no attempt was made to use an instantaneous strain rate effect varied spatially throughout the structure. Therefore, a comparison of peak and permanent deflection provides the best basis for assessing the accuracy of the models.

A comparison of measured and predicted peak and permanent strains is shown in Fig. 5. Peak and permanent deflection at the end of the tube and at the end of the torque arm are compared in Fig. 6. These comparisons show that the behavior is being predicted reasonably well, although there is considerable scatter in the data.

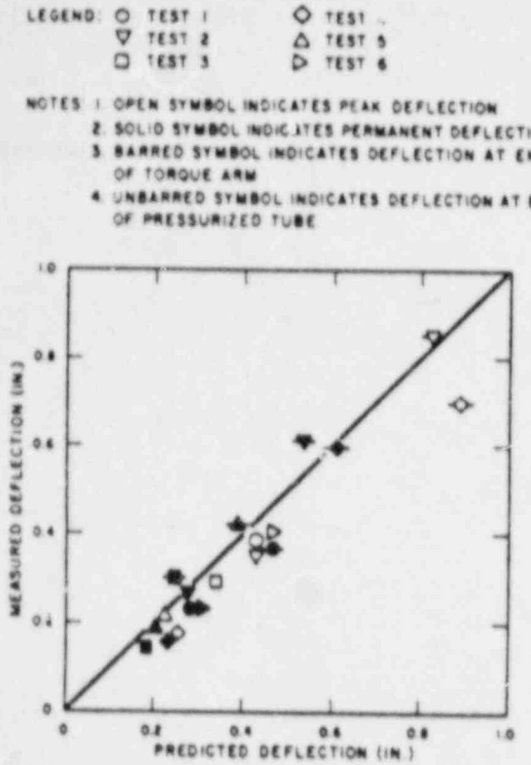

Fig. 6 Comparison of predicted and measured deflections

Discussion

Usually the data from dynamic tests, especially those in which plastic deformation occurs, show greater scatter than those obtained from static tests. Based on survey results, Baker [5] reported a minimum and maximum scatter of ± 29.4 percent and ± 67.3 percent, respectively, for permanent deformation of well-controlled cantilever beam tests. The spread in the data reported here is generally within ± 25 percent of the predicted value although some points are outside this band.

The correlation of analytical predictions and experimental results shown here along with the correlations for static loading previously reported in reference [2] demonstrate that the basic approximation for a tube or pipe element used to reduce a complex three dimensional problem to a simple beam problem give reasonable results. There are several potential applications for the approximate model. Since the inelastic dynamic response of a pressurized piping system is an extremely complex problem, the degree and type of approximation used will ultimately depend on the particular problem and the desired result. For complex systems, approximate models such as discussed here could be very useful in identifying what cross section in the structure will undergo gross yielding during a transient. These locations could then be studied in more detail by refined methods if required.

Summary and Conclusions

The approximate model for analysis of the inelastic deformation of a tube element under combined loading has been applied to the prediction of the dynamic inelastic behavior of tubes. The predictions of peak strains and deflections agreed reasonably well with the measured results for a number of different tube dimensions and loading combinations. On the basis of these results, it is concluded that the approximate model is a useful tool for the analysis of dynamic loading involving significant inelastic deflection.

References

1 *Boiler and Pressure Vessel Code*, ASME, Section III, 1971 edition, p. 101, par. NB-3225.

2 Larson, L. D., Stokey, W. F., and Fransen, W. E., "An Approximate Model for an Elastic-Plastic Pipe Element Under Combined Loading," JOURNAL OF PRESSURE VESSEL TECHNOLOGY, TRANS. ASME, Vol. 97, Series J, No. 1, Feb. 1975, pp. 22-28.

3 Biggs, J. M., *Introduction to Structural Dynamics*, McGraw-Hill Book Company, 1964.

4 Larson, L. D., "Inelastic Response of Pressurized Tubes Under Dynamic Bending and Torsional Loads," PhD thesis, Mechanical Engineering Department, Carnegie-Mellon University, 1973; University Microfilm Order No. 73-22872.

5 Baker, W. E., "Validity of Mathematical Models of Dynamic Response of Structures to Transient Loads," *The Shock and Vibration Bulletin 41*, Part 7, Dec. 1971, pp. 19-28, N72-16845.

APPENDIX

As developed in reference [2] the equations for the bending and torsional deformation of an element of tube when the bending moment and torque are varied, the pressure and axial force being constant, are:

$$d\varphi_1 = (A_{11} + B_{11})dQ_1 + (A_{14} + B_{14})dQ_4 \tag{12}$$

$$d\varphi_4 = (A_{41} + B_{41})dQ_1 + (A_{44} + B_{44})dQ_4 \tag{13}$$

where $\varphi_1 = \frac{2}{\pi} RK$

$\varphi_4 = \frac{R}{\sqrt{3}} K_{xt}$

R = mean radius of tube

K = tube curvature

K_{xt} = angle of twist per unit length

$A_{11} = \frac{8}{\pi^3 E}$

$A_{14} = A_{41} = 0$

$A_{44} = \frac{2(1+\nu)}{3E}$

$B_{11} = \frac{C}{F^3 \cos^3 \theta_n} \left(\frac{Q_1}{Q_n} \right)^3$

$B_{14} = B_{41} = \frac{C}{F \cos \theta_n} \frac{Q_1 Q_4}{Q_n^3}$

$B_{44} = \frac{C Q_4^3}{Q_n^3}$

$Q_n = \left[\left(\frac{Q_1}{\cos \theta_n} \right)^3 + \frac{3}{4} (Q_2 - Q_3)^3 + Q_4^3 \right]^{1/3}$

$\theta_n = \frac{(2Q_2 - Q_3 - Q_3)}{\sqrt{Q_4^3 - \frac{3}{4}(Q_2 - Q_3)^3 - Q_3^3}} \frac{\pi}{4} \qquad |\theta_n| < \frac{\pi}{2}$

θ_n = angle defining location of neutral axis

$Q_1 = M/4R^2h$, generalized bending stress

$Q_2 = N_x/h$, generalized hoop stress

$Q_3 = -p/2$, generalized radial stress

$Q_4 = \sqrt{3}T/2\pi R^2 h$, generalized shear stress

$Q_5 = N_x/2\pi Rh$, generalized axial stress

Q_e = generalised effective stress of the cross section

N_t = hoop stress resultant

p = internal pressure

M = applied bending moment

T = applied torque

N_z = axial force

$q_e^p = \left(\frac{Q_e}{C_1}\right)^{C_2}$ is, the strain hardening curve which can be obtained from a simple tension test

$$C = \frac{dq_e^p}{dQ_e} = \frac{C_2}{C_1}\left(\frac{Q_e}{C_1}\right)^{C_2-1}$$

$$F = \cos\theta_e + \theta_e \sin\theta_e$$

Substituting the expressions for q_1, q_2, Q_1, and Q_2 into equations (12) and (13) and simplifying yields:

$$dK = (A_{11} + B_{11})\frac{\pi}{8R^3h}\,dM + (A_{12} + B_{12})\frac{\sqrt{3}}{4R^2h}\,dT$$

$$dK_{xz} = (A_{21} + B_{21})\frac{\sqrt{3}}{4R^2h}\,dM + (A_{22} + B_{22})\frac{3}{2\pi R^2h}\,dT$$